Journal of Engineering Mathematics **50:** 157–175, 2004.

Surfactant-driven motion and splitting of droplets on a substrate

L.W. SCHWARTZ*, R.V. ROY, R.R. ELEY[1] and H.M. PRINCEN[2]
Department of Mechanical Engineering, University of Delaware, Newark, DE 19716, U.S.A.; [1]*ICI Paints Research Center, Strongsville, OH 44136, U.S.A.;* [2]*Consultant, Surfaces & Colloids, Flemington, NJ, U.S.A.*

Received 12 December 2003; accepted in revised form 25 June 2004

Abstract. A theoretical and computational model is presented to predict the motion of a small sessile liquid droplet, lying on a solid substrate including surfactant effects. The model, as formulated, consists of coupled partial differential equations in space and time, and several auxilliary relationships. The validity of the long-wave, or 'lubrication' approximation is assumed. It is shown that there are circumstances where surfactant injection or production will cause the droplet to split into two daughter droplets. It is conjectured that the results are relevant to basic mechanisms involved in biological cell division (cytokinesis). It is also demonstrated that motion of a droplet, analogous to the motility of a cell, can be produced by surfactant addition. Computed examples are given here, in both two and three space dimensions. Approximate energy requirements are also calculated for these processes. These are found to be suitably small.

Key words: cell division, coupled partial differential equations, lubrication approximation, numerical model, surfactant theory

1. Introduction

This paper is concerned with the flow of liquids in thin layers, especially when the liquid contains surface-active ingredients, *i.e.*, surfactants. Surfactants find use in the chemical-process industries, food and personal care products, pharmaceuticals, agrochemicals, and elsewhere [1, 2]. Unanswered questions in cell biology are another motivation for this study. This work lends support to the theory that there are processes of cell division that depend on the production and controlled release of surfactant within cells.

There is a strong analogy between soap films and the bilipid membranes or lipid bilayers that form the 'skin' of living cells. Structurally, a soap film consists of two interfaces, each of which joins an internal liquid phase with an external gas phase. Thus, two similar gas phases are separated by a thin lamella of liquid. This lamella can become very thin, of the order of 5 to 10 nm for so-called 'black' films [3]. In order to prevent ultimate rupture, the two interphase boundaries must repel each other. This repulsion is usually much larger when surfactant is on these interfaces. Operationally, sufficient surfactant must lie on the interfaces for thin liquid membranes to persist for appreciable times. Similarly, the simplest enclosure for a cell must also be a two-sided membrane since both the inside of the cell and the exterior environment are aqueous phases. The cell membrane may be thought of as a very thin oily or fatty liquid layer whose structure is largely determined by the properties of the opposing surfactant molecules on the two interfaces.

The density of surfactant molecules on the interface between immiscible fluids need not be constant. Important dynamical properties of thin liquid films are caused by nonuniform

*Author to whom correspondence should be addressed. Email: Schwartz@me.udel.edu

surface concentration of surfactant. Interfacial or surface tension σ is a decreasing function of concentration; thus, if the surface concentration decreases in a certain direction along an interface, there will be a net force on an element of interface in that direction. If the motion is slow, or the dimensions of the physical system are small, this net force must be balanced by a traction force exerted on the interface by the adjacent liquid. From the point of view of the liquid, therefore, a spatial variation of surface concentration c is equivalent to an applied surface tangential stress, that, in the simplest case, is given by

$$\tau = \frac{\mathrm{d}\sigma}{\mathrm{d}x} = \frac{\mathrm{d}\sigma}{\mathrm{d}c}\,\frac{dc}{dx}\,. \tag{1.1}$$

These surface tractions, or *Marangoni stresses*, drive liquid flow, causing convection, extension and distortion of interfacial area elements. As the interface moves, the surfactant distribution also changes, resulting in changes in the traction field. Thus, fundamentally, it is necessary to solve a coupled system of equations in space and time, including all other body and surface forces, to determine what the effect of surfactant will be in any given situation. For surfactants of appreciable solubility, molecules move to and from the interface into the bulk liquid. This transfer, as well as the transport of surfactant within the bulk of the liquid, would need to be included in a complete model. The presence of surfactant will also change the magnitude of the pressure jump across curved interfaces and can lead to additional pressure gradients within the bulk liquid film. For thin films, however, this pressure effect is typically much less important than the development of shear stresses. By comparing model computational results with experimental observation, we have demonstrated that surfactant-induced Marangoni stresses are responsible for certain defects, called 'craters', in drying paint films [4]. It should also be noted that Marangoni stresses can arise from other causes; an important example is surface-tension changes due to local compositional changes in the bulk liquid beneath the surface. This is the source of the 'wine tears' phenomenon and is also relevant to the drying behavior of certain paints [5, 6].

These problems are very complex, involving the motion of fluid-phase boundaries, surfactant transport, other necessary physicochemical influences as well as geometric considerations. A general mathematical description is not possible and judicious approximation is necessary. The basis of the approximations used here rests on the thinness of the liquid films, the assumption of slow flow, as well as the assumption of slow variation along the film. The last of these is also called a long-wave approximation. Together, these simplifications constitute the free-surface *lubrication approximation* [7–9]. These simplified models can be analyzed in two complementary ways. Asymptotic and perturbation methods can be used to find approximate solutions in limiting cases; these cases would typically use extreme values, *i.e.*, very large or very small values, of one or more input parameters. Several groups have formulated and solved two-dimensional mathematical models for thin liquid films with surfactant effects. The work was motivated by either biomechanical or industrial applications [10, 14]. For the most part, however, we will use direct numerical solution of the governing set of coupled partial differential equations for time-dependent three-dimensional problems. We have available highly-efficient computer algorithms for these systems. Typically, we use alternating-direction implicit (ADI) methods [15, 17].

Perhaps the most important study area concerns the search for mechanisms that are used by living cells. Aspects include the control of cell division and self-propulsion, or *motility*. Here we will give model results for the behavior of a small droplet on a substrate in the presence of surfactant. We demonstrate that there are circumstances where surfactant injection

or production will cause the droplet to split into two daughter droplets. We believe that these results are relevant to basic mechanisms involved in biological cell division (cytokinesis).

The idea that cell division is driven by surfactant release within a living cell is at least 100 years old. The analogy between cells and droplets was advocated strongly in the fluid mechanics community by H.P. Greenspan in the 1970s [18–21]. Greenspan's work includes studies of both free-floating and sessile drops, although he only considered surfactant effects in the former case. It seems that this rather simple theory has been de-emphasized in favor of proposed more complicated mechanisms. After more than a century of study, it is still correct to say that there is no universally accepted causative mechanism for cell division [22]. We believe that the downgrading of the surfactant theories stemmed from the inability of any previous mathematical model to simulate the cleavage process, even though cleavage of droplets by surfactant has been shown to work in the laboratory. Our new model appears to mimic the cleavage of droplets and cells. We believe that previous models failed because the all-important transport of surfactant was not considered.

We are concerned with the specific situation where cells, in culture for example, adhere to walls. For these cells, as for attached droplets, it is necessary to include, in the model, the energetics of adhesion. We do this through use of so-called *disjoining pressure*. Disjoining pressure is an effect for thin liquid films that was discovered originally by the Russian chemical physicists Frumkin and Deryaguin in the 1930's [23–25]. It allows information about the three interfacial energies, in the neighborhood of the so-called three-phase contact line where the liquid, vapor and solid substrate meet, to be combined with capillarity and other sources of pressure. In particular, an energetically-favored equilibrium contact angle, at the contact line, can be specified. While originally used only for static problems involving liquids on substrates, disjoining pressure has recently been incorporated in dynamic models by us and others [26–30]. Suitable disjoining models allow a liquid front both to advance onto, and to recede from, a sensibly-dry solid surface. Prescription of a very thin wetting film or slip film thickness allows theoretical difficulties with moving contact lines to be overcome [31].

In 1918 Spek succeeded in cleaving a neutrally-buoyant drop of oil using surfactant. He offered this demonstration as evidence for the surfactant theory of cell division [32]. Unfortunately, a number of details of Spek's experimental procedures were not reported. The experiment was repeated more recently by Greenspan using a different oil and simultaneous deposition of NaOH at opposite poles of the circular droplet [18, 20]. Reaction of the caustic solution with the oil forms soap, *i.e.*, surfactant. Greenspan reported significant difficulties before he finally found a particular method for successful cleavage. Guided by Greenspan's work, we have also been able to cleave a free floating droplet in the laboratory. We have made videos of droplet cleavage using a oil drop in water. Our oil is an equal-parts mixture olive oil, cod liver oil, and chloroform. The last component was used to reduce the viscosity of the mixture. We also used a sodium hydroxide solution to produce the cleavage.

No complete theoretical or computational model has appeared for the oil-drop cleavage process, although Greenspan offers a partial mathematical model using perturbation techniques [19]. Greenspan's model assumes the drop is axisymmetric with surfactant introduced at the poles. Splitting is expected at the equator. He and Dembo perform finite-element simulation with Greenspan's geometry [33]. Their model assumes a surface tension distribution that is a given fixed function of axial position. This distribution makes the pressure within the drop nonuniform as well as producing a surface shear stress or traction distribution. Over a wide range of assumed surfactant distributions, they find that the drop shape reaches a steady state with only a small contraction at the equator. They are only able to cleave a drop by reducing

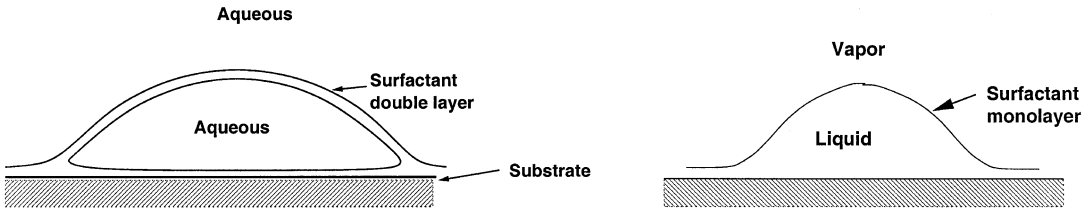

Figure 1. Simplified schematic models of a cell attached to a substrate (left) and a sessile drop (right). Each can be moved and distorted by surface tension gradients produced by spatially nonuniform surfactant distributions. The theoretical model used here to calculate the motion is applicable to either situation. A thin 'slip layer', greatly exaggerated here, allows contact-line motion.

the traction while leaving the pressure distribution unchanged. They justify this reduction by invoking a transport effect of unknown origin. Similarly, earlier computational work of Zimmerman and Nir also assumed a surface tension distribution and was likewise unable to demonstrate cleavage [34]. These difficulties were likely to have discouraged other workers because they seem to suggest that surfactant cleavage theories are, at best, quite incomplete.

We will demonstrate that surfactants are much more effective than the above cited computations would suggest. In fact, the motions induced by releasing surfactant to the droplet interface or cell boundary will carry the surfactant to locations where its effectiveness is enhanced. These are inherently nonlinear effects that cannot be realized in the above-cited calculations. In our calculations we find that it is necessary for the source of surfactant to be allowed to move with the deforming liquid, in order to achieve complete cleavage.

The relevant geometry, for either cells or drops, is shown schematically in Figure 1. The cell is thought to behave in a manner similar to a sessile drop on a solid substrate that makes a finite contact angle with the substrate when it is at rest. Because, for the cell, inner and outer phases are both aqueous, it is necessary for the cell membrane to be a double interface or bilayer. Surfactant is present in either case. One obvious difference is easily accommodated; because there are two interfaces, the film tension, for the cell, is twice the surface tension that would be measured if there were only a monolayer. There is significant evidence that certain cells behave like water droplets. Carter reports that cells, when placed on a substrate where the equilibrium contact angle for water has been made to vary, will migrate in the direction of smaller contact angle [35]. This is exactly the behavior that is observed for a water droplet on such a surface.

The conjectured cell-splitting mechanism is illustrated schematically in Figure 2. The figure is a top view of a droplet or cell that is initially circular when viewed from above. The two black spots are locations in the cell where surfactant is to be released or inserted onto the interface or cell membrane. Surface tension is lowered by the surfactant release and the cell membrane experiences a net tension that will pull it inward towards the center. As the membrane moves, it carries the previously released surfactant with it. In addition, the sources of surfactant are particular moieties that are parts of the cell. As the 'waist' contracts, therefore, the sources of surfactant release are brought inward. Because the surface concentration of surfactant is now larger near the center of the cell, the surface-tension-gradient or Marangoni force pulls liquid to the two eventual daughter cells. The Marangoni force will also cause the two developed nascent daughters to move apart from one another. We will demonstrate in Section 3 below, using our mathematical model, that this sequence of events, with relatively slow and continous surfactant release, is a very efficient path to cleavage. It is more efficient,

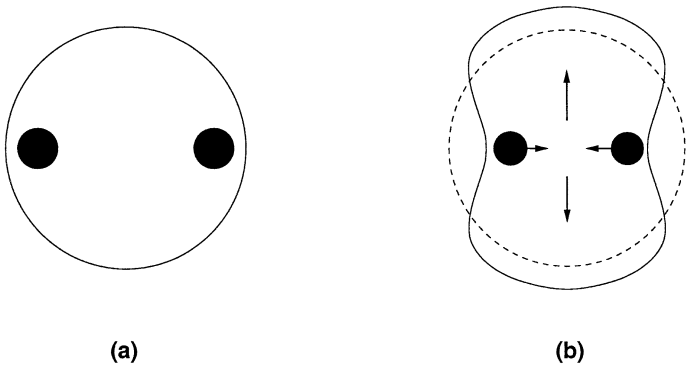

Figure 2. Top views of a deforming drop or cell (conceptual): The surfactant is released at two locations within the moving and deforming cell, leading to splitting; (a) Original shape; (b) Original and distorted shapes superimposed. The big dots represent moving surfactant sources. The arrows show the direction of Marangoni-stress-driven flow. The surfactant sources are material particles within the cell and are moved inward with the average flow velocity, because of the net force that the release produces. This Marangoni flow both constricts the waist and drives the vertical stretching flow. If the surfactant release is done in a particular manner, the drop will split.

for example, than a heat-producing chemical reaction that might also be used to produce Marangoni forces.

Another intriguing observation, made some years ago by several groups, was that surfactant addition to the environment of dividing cells immediately stops the cell division [36]. One result of our energy model is that a uniform addition of surfactant everywhere on the surface will lower the amount of stored energy. This lowering might be sufficient to remove the possibility of subsequent division. This seems to be consistent with, and provides a possible explanation for, the experimental observation. It is interesting to note that this experimental result caused a flurry of excitement during the 1950's. It was thought, in some quarters, that a way might be found to use surfactant as a way to stop the uncontrolled cell division in the spread of cancer.

2. The Mathematical model for droplet motion with surfactant

The equations of motion for a viscous liquid region lying on a solid substrate can be considerably simplified if the slope of the uppermost moving boundary of the liquid is uniformly small with respect to the nominally planar substrate. Using the long-wave or lubrication approximation, the three-dimensional evolution equation for $h(x, y, t)$, the shape of the liquid-air interface, becomes

$$h_t = -\nabla \cdot \mathbf{Q} = \frac{1}{3\mu}\nabla \cdot (h^3 \nabla p) - \frac{1}{2\mu}\nabla \cdot (h^2 \nabla \sigma) \; . \tag{2.1}$$

Here $\mathbf{Q}$ is the flow rate and μ is the assumed-constant viscosity. The terms on the right represent pressure driven and surface traction driven flows, respectively. The applied shear stress or traction is equal to the gradient of the surface tension σ [37]. An equation equivalent to (2.1), governing the combined motion and employing the lubrication approximation, is used by Levich [38] and, more recently, by a number of others. The pressure p is given by a combination of capillary pressure and so-called 'disjoining pressure':

$$p = -\sigma \nabla^2 h - \Pi = -\sigma \nabla^2 h - \frac{B}{h_*}\left[\left(\frac{h_*}{h}\right)^n - \left(\frac{h_*}{h}\right)^m\right] \tag{2.2}$$

where

$$B = \frac{(n-1)(m-1)}{(n-m)}\,\sigma(1-\cos\theta_e) \approx \frac{(n-1)(m-1)}{2(n-m)}\sigma\ \theta_e^2\ . \tag{2.3}$$

Here θ_e is the equilibrium contact angle and the small-slope approximation has been invoked again. The ∇-operator is two-dimensional, and is written using the substrate coordinates. The first term in (2.2) uses the small-slope approximation to the surface mean curvature while the second is a two-term model of disjoining pressure Π that allows contact-line motion. Here h^* plays the role of a 'slip coefficient'. B, h^*, m, and n are positive constants with $n > m$. For the results presented here, we will take $m = 2$ and $n = 3$ but the results are not very sensitive to the choice of exponents [28, 29]. The disjoining pressure is seen to be zero when $h = h^*$. By definition, the disjoining pressure is the derivative of the additional surface energy E with respect to normal displacement of the thin wetting layer, *i.e.*, $\Pi = -\mathrm{d}E/\mathrm{d}h$. More physically, the added pressure changes from repulsive for $h < h^*$ to attractive for $h > h^*$, thus a 'thin slip layer', of thickness $h = h^*$, is energetically favored. The layer has the ability to re-establish itself after the imposition of a transient force, for example. The disjoining pressure difference, between the thin wetting layer and the interior of a static drop, is available to balance the capillary-pressure contribution that favors spreading. This leads to a finite stable drop exhibiting a particular contact angle [23, 24, 1].

When a drop moves on a dry surface, the no-slip condition must be abandoned in the immediate vicinity of the three-phase or 'contact' line. If this were not done, the work required to move the contact line would be infinite [31]. Several 'slip' models, involving a free parameter, have been used. The present simulations use a wetting layer to overcome the 'contact-line paradox'. Thus within the model, the substrate is never truly dry anywhere. The wetting-layer plays the role of a slip parameter. Comparisons between wetting layer models and slip models are given in [9]. Each type of model can be used either with or without disjoining pressure. With disjoining pressure, as used here, the droplet has a finite dynamic contact angle that will be maintained as the 'wetting line' recedes. Thus de-wetting is simulated by the model. Without disjoining pressure the receding contact angle is zero; thus the liquid will not de-wet and cannot leave behind a sensibly dry substrate.

The surface tension variation in the model is due to changes in surface concentration c of a surfactant. We assume a simple linear law,

$$\sigma = \sigma_0 - K\ c\ . \tag{2.4}$$

While any smooth law $\sigma(c)$ can be approximated locally by an appropriate choice of constant K, use of the linear law imposes the additional requirement that the changes in surface tension are relatively small. Consequently a surface shear stress τ, that is due to nonuniform distribution of surfactant, is available to drive liquid motion and is given by

$$\tau = \nabla\sigma = -K\ \nabla c\ .$$

Thus Equation (2.1) involves the two unknown fields $h(x, y, t)$ and $c(x, y, t)$. A second coupled equation is thus required for the simultaneous determination of these fields. Note that an improved model can use a more general relation for $\sigma(c)$ to replace Equation (2.4). When surface tension changes are large, a more general law is indicated. Such a law has been incorporated in numerical simulation by Evans *et al.* [4].

The surfactant concentration satisfies a convection diffusion equation, which may be approximated by

$$c_t + \nabla\cdot(\mathbf{u}^{(s)}c) = D\nabla^2 c - D_b\ c + I(x, y, t). \tag{2.5}$$

Apart from the last two terms on the right side of (2.5), the exact form of the concentration equation is given by Stone [39], and further clarified by Wong *et al.* [40]. We note that terms involving the reduction in concentration due to normal motion of the free surface have been omitted from (2.5). This omission can be justified for thin-layer flows. $\mathbf{u}^{(s)}$ is the vector surface velocity and is parallel to the substrate in the thin-layer approximation [41]. The first two terms on the right are surface diffusion of surfactant and a general dissipative loss of surfactant which is essentially equivalent to a simplified transfer or 'diffusion' of surfactant into the bulk liquid. The function I represents introduction of surfactant to the surface as a function of space and time. This 'self injection' of surfactant is the key to droplet or cell cleavage.

If only c_t and the D_b terms in (2.5) are considered, the action of D_b becomes clear. It causes surfactant to be lost from the free surface at a rate proportional to the instantaneous value of c. The D_b term gives a finite lifetime for surfactant activity. The effective time constant is D_b^{-1}. We note that this simple loss mechanism for surfactant could be improved upon in a more complete model. The transfer rate of surfactant to the bulk liquid could be proportional to an effective concentration difference and the advection of surfactant in the bulk liquid would need to be calculated as the solution of another coupled equation [38].

The boundary conditions on the computational domain A of the (x, y) plane are reflection symmetry, *i.e.*,

$$\mathbf{Q} \cdot \mathbf{n} = \nabla h \cdot \mathbf{n} = \nabla c \cdot \mathbf{n} = 0 \,, \qquad \text{on } \delta\mathrm{A}, \tag{2.6}$$

where δA denotes the boundary of A and $\mathbf{n}$ is an outward unit normal vector. The boundary condition (2.6) says that liquid volume is conserved. In addition, there is no loss or gain of surfactant through the computational boundaries. The only mechanism for surfactant loss is diffusion to the bulk via the D_b term.

The model system of equations will now be reduced to dimensionless form. Our initial or reference state is a sessile drop with a well-defined static or equilibrium contact angle θ_e. The film thickness reference dimension h_0 is the initial centerline height of the static drop. In light of the small-slope approximation and the neglect of gravity, the drop is a paraboloid that satisfies $\nabla^2 h = 0$. We let L, the substrate reference length, be the drop radius. Then the equilibrium contact angle is

$$\theta_e \approx \tan\theta_e = \frac{2h_0}{L}.$$

Both pressures p and Π are measured in units of $\sigma_0 h_0/L^2$. where σ_0 is the surface-tension value for a 'clean' interface. The fractional change in surface tension $\Delta\sigma/\sigma = -K\,\Delta c/\sigma_0$ is assumed small so that $\sigma \approx \sigma_0$ in the capillary pressure term in (2.2).

The reference time is taken to be

$$T^* = \frac{3\mu L^4}{\sigma_0 h_0^3} \tag{2.7}$$

and two parameters that appear in the model are a dimensionless measure of surfactant strength R and a dimensionless surface-diffusion coefficient for surfactant $\tilde{D}$. These are given by

$$R = 3\,\frac{K}{\sigma_0}\,\left(\frac{L}{h_0}\right)^2, \qquad \tilde{D} = DT^*/L^2. \tag{2.8}$$

In these units, the dimensionless form of the surface evolution equation is

$$h_t = -\nabla \cdot \left[h^3 \nabla \left(\nabla^2 h + \Pi\right)\right] + \frac{R}{2}\,\nabla \cdot (h^2 \nabla c)\,. \tag{2.9}$$

while the concentration satisfies

$$c_t + \nabla \cdot (\mathbf{u}^{(s)} c) = \tilde{D}\ \nabla^2 c - \tilde{D}_b\ c + I(x, y, t). \tag{2.10}$$

The nondimensional $\tilde{D}_b$ is measured in units of $(1/T^*)$. The dimensionless surface velocity is given by

$$\mathbf{u}^{(s)} = -Rh\nabla c + \frac{3}{2}h^2\nabla\left(\nabla^2 h + \Pi\right)\ . \tag{2.11}$$

The surface velocity can be seen to be the linear combination of a 'Couette' term, driven by a shear stress that is proportional to the surfactant concentration ∇c, and a 'Poiseuille' term that is proportional to the gradient of the total pressure. Finally, using the disjoining exponents $(n, m) = (3, 2)$, we have

$$\Pi = \frac{4}{h^*}\left[\left(\frac{h^*}{h}\right)^3 - \left(\frac{h^*}{h}\right)^2\right]\ . \tag{2.12}$$

3. Model results for splitting

The model given above has been translated into a computer algorithm using the Fortran language. The coupled system of equations is solved by a partially-implicit time marching method. Details of the algorithm, for a closely-related axisymmetric problem with surfactant, are given by Evans *et al.* [4]. Some algorithm details, for a three-dimensional problem with an evolving free surface with Marangoni effects, may be found in [42]. In that work the Marangoni effect arises from changes in liquid concentration, rather than presence of surfactant. In both [4] and the present work, the spatially fourth-order surface evolution equation and the second-order concentration equation, are solved by alternating implicit 'sweeps' in the substrate coordinate directions. In each calculation, fourfold symmetry has been assumed.

Rendered pictures, or 'frames', from our computer simulations are shown in Figures 3–5. The first frame shows a small amount of pinching at the waist and happens shortly after surfactant release begins. Steady release continues until the daughter droplets are almost formed. Surfactant release is then stopped. The residual surfactant concentration gradients gives the Marangoni forces necessary to complete the separation. Parameters have been chosen to simulate cleavage of white blood cells or leukocytes to the extent that the relevant quantities are known. Thus each cell or droplet has a diameter of 10 μm and the division takes place in several minutes. The membrane tension is taken to be 1·0 dyne/cm; this is consistent with values measured by Harvey [43] and Hochmuth [44].

In dimensionless units, a surfactant source of radius $r_0 = 0{\cdot}15$ is initially located at $x_0(0) = 0{\cdot}8$. The injection function is

$$I(x, y, t) = C(t)\ \left[1 + \frac{(x - x_0(t))^2 + y^2}{r_0^2}\right]^{-10} \tag{3.1}$$

Taking the exponent to have the large value 10 yields an injection profile that is almost constant within the moving source and quite small away from the source. In each case shown in the figures, the surfactant strength parameter is $R = 100$ in (2.8). The bulk loss coefficient $\tilde{D}_b$ in (2.10) was taken equal to five for the first two cases. The rate of surfactant supply, $C(t)$ in (3.1), was taken to be constant until turned off.

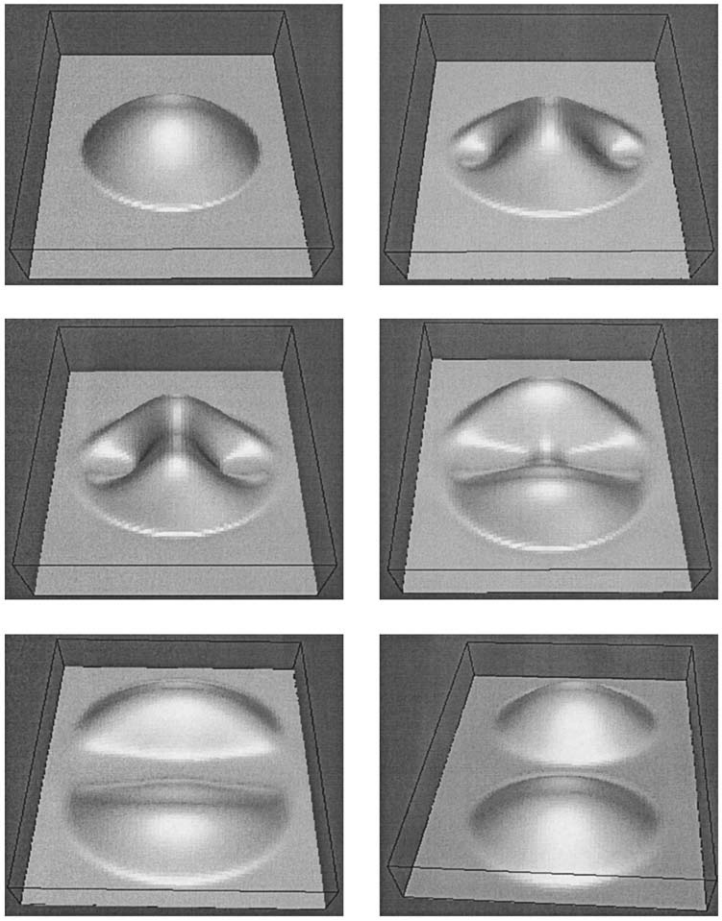

Figure 3. Rendered pictures of the numerical simulation of drop splitting. Read across, then down. Dimensionless surfactant delivery rate is $C = 100$. Dimensionless times are 0·001 (almost relaxed drop at start of injection), 0·02, 0·04, 0·075 (end of surfactant delivery), 0·2, 0·9. Two smaller drops at the equilibrium contact angle are shown at the last time. The surfactant has dissipated.

A successful splitting sequence in shown in Figure 3. Until it is stopped, the injection rate has the large value $C = 100$. As the droplet contracts along a line connecting the two symmetrically placed surfactant sources, these sources move inward. They remain positioned under the point x_0 on the substrate where $h(x_0, 0, t) = 0{\cdot}15$. The source supply rate $C(t)$ is turned off when x_0 reaches 0·1. The drop is seen to distort significantly in response to the large surface-tension gradient forces. The surface diffusion constant is $\tilde{D} = 0{\cdot}5$ and the slip thickness is $h^* = 0{\cdot}05$. The drop breaks relatively quickly. The surfactant supply turns off at dimensionless time equal to 0·075. The surfactant gradient on the surface is sufficient to complete the split which happens soon thereafter. The two daughters move apart and relax to their equilibrium shapes. The process is completed before $t = 1$.

Figure 4 shows results for the much lower supply rate $C = 5$. This is just about the minimum rate of supply that will split the drop. There is no severe deformation as was shown in the previous figure. One may say that the drop splits 'quasi-statically' in the sense that the daughters remain roughly paraboloidal during much of the process. The rate of deformation

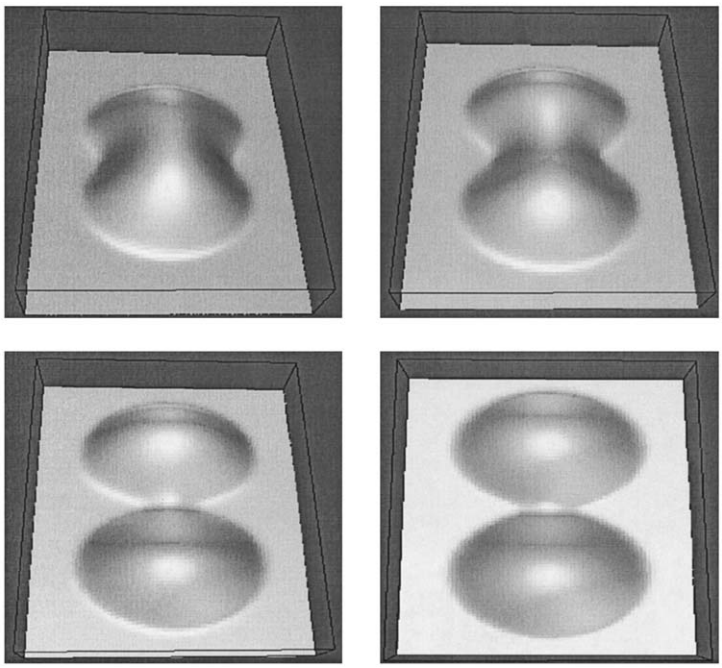

Figure 4. Simulation of drop splitting using a lower rate of surfactant delivery. Drop breaks almost quasi-statically. Delivery rate $C = 5$. Dimensionless times shown are 0·5, 1·0, 1·5 and 1·8.

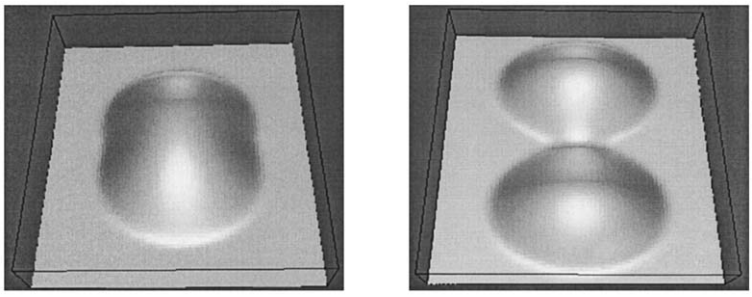

Figure 5. Two incompletely cleaved drops. Left: A steady-state solution with continuous surfactant injection. The rate of injection $C = 1$ is just sufficient to maintain a steady-state surface tension gradient to hold the drop in a constricted form, but is insufficient to cause cleavage. Other parameter values are $R = 100$, $\tilde{D} = 0{\cdot}5$ and $\tilde{D}_b = 0$. Right: Larger injection rate $C = 5$, but the surface diffusion constant has been increased to $\tilde{D} = 2$. Surfactant injection becomes intermittent as the droplet waist oscillates about the cut-off position. Both these profiles correspond to long times and large values of injection work and total injected surfactant.

is essentially proportional to C. Thus the drop reaches the critical deformation $x_0 = 0{\cdot}1$ more slowly by a factor of twenty than in the previous figure.

Figure 5 shows less successful splitting attempts. The left half of the figure shows a steady-state situation for a low rate of delivery $C = 1$. Here the loss of surfactant effect is due solely to surface diffusion with no loss to the bulk, *i.e.*, $\tilde{D}_b = 0$. The model does not currently consider reduction in the average level of surface tension; thus all situations where the surfactant is uniformly distributed in the computational window are equivalent. Hence the diffusional loss of effect, with $\tilde{D} = 0{\cdot}5$, exactly balances the supply of new surfactant. The surfactant-gradient field becomes steady which is equivalent to a time-invariant surface traction field. The

constricted shape shown will persist as long the supply is maintained. Mathematically, this demonstrates that the model system (2.9–12) admits non-trivial stable steady-state solutions. Because $\mathbf{u}^{(s)}$ is nonzero, the steady configurations have internal circulation.

The right-hand picture in Figure 5 is a snapshot from a periodic cycle of deformation. Here the supply rate has been increased back to the earlier value $C = 5$ and the diffusion coefficient is $\tilde{D} = 2$. Periodicity is due to the shut-off of surfactant when x_0 becomes as small as 0·1. The drop then begins to return to its starting shape; however the supply is turned on as x_0 increases past 0·1. The surface-tension gradient takes some time to build up sufficiently for the drop to again begin to contract. This illustrates that the mathematical model, as constructed here, encompasses the ability to produce cyclical motions.

4. Energetics

Recently we have derived expressions for the potential or stored energy for an interface with nonuniformly distributed surfactant [45]. There is a minimum amount of work that must be done by the cell to create this nonuniform distribution. This stored energy is then used to overcome viscous resistance and also to create the increased surface area of the daughter droplets. One check on the reasonableness of the proposed cell division mechanism is to express this energy budget as the equivalent temperature increase of the cell liquid volume using the specific heat of water. We expect that the temperature rise should be significantly less than one Celsius degree. The particular process we identify here is only one of many dissipative processes that probably occur. Nevertheless, it is necessary that this process not be overly 'expensive'.

Other surfactant release histories were also tried using the numerical model. Higher rates of surfactant release, that are continued until the drop has almost split, will also work. The cell or drop splits more quickly. The drop became much more distorted, however; this rough treatment may not be suitable for living cells. Moreover the required energy budget, as discussed above, is higher by a factor of ten or more.

Within the small-slope approximation, the total stored or potential energy for a droplet without surfactant is divided between surface energy E_σ and 'disjoining energy' E_d. The latter measures the work done against the disjoining pressure to raise each element of the free surface from its energy minimum, at a layer thickness of $h = h^*$, to its actual location. Each of these two energies depends on the detailed shape of the droplet. Further information about the energies E_σ and E_d can be found in [29]. With no surfactant, or with uniformly distributed surfactant, the stable sessile-drop configuration corresponds to a minimum of the energy sum $E_\sigma + E_d$. The surface energy, representing the increased surface area of a raised drop, relative to a perfectly flat interface, is

$$E_\sigma = \frac{\sigma}{2} \iint \nabla h \cdot \nabla h \ \mathrm{d}A \tag{4.1}$$

with an error of $\mathrm{O}(|\nabla h|^4)$ in each surface area element. Here A is the area of the computational domain. The disjoining energy is

$$E_d = \iint e^{(d)} \ \mathrm{d}A \tag{4.2}$$

where

$$e^{(d)}(h) = -\int_{h^*}^{h} \Pi(\eta)\, \mathrm{d}\eta = \frac{\sigma}{2}\,\theta_e^2\,\left(1 - \frac{h^*}{h}\right)^2 \tag{4.3}$$

and energy density $e^{(d)}$ uses the exponent pair $(n, m) = (3, 2)$ in Equation (2.2) [29]. Since $h \gg h^*$ on the drop and $h \approx h^*$ on the 'unwetted' portions of the substrate, the disjoining energy is approximately equal to the constant $(\sigma/2)\,\theta_e^2$ times the footprint area of the drop or drops. As reference values, for a paraboloidal droplet on a flat substrate, and assuming that the central height h_0 of the paraboloid is much larger than the slip thickness h^*, these energies are

$$E_\sigma = \pi\sigma h_0^2\,, \qquad E_d = 2\pi\sigma h_0^2\,. \tag{4.4}$$

Any stable configuration, for a given liquid volume, corresponds to a local minimum value of $E_\sigma + E_d$. These stable configurations consist of one or several isolated axisymmetric drops. The absolute minimum-energy configuration will have all the liquid in a single drop. Thus making two drops from one will require input work.

Another type of potential energy is the stored energy associated with a non-uniform surfactant distribution $c(x, y, t)$ [45]

$$E_c = K\,c_0 \iint \frac{c}{c_0}\,\log\frac{c}{c_0}\,\mathrm{d}A_1 \tag{4.5}$$

where $K = -\mathrm{d}\sigma/\mathrm{d}c$, as given in equation (2.4). It is perhaps surprising that the energy associated with the surfactant distribution cannot be calculated simply from

$$E_0 = \iint \sigma\,\mathrm{d}A\,.$$

However it is easy to see, for a given total quantity of surfactant and with the linear law for $\sigma(c)$, that the energy E_0 is constant. It is quite independent of how the surfactant is distributed. The law in (4.5), on the other hand, derives from consideration of the work done against Marangoni stresses as the nonuniform distribution is established, starting from an initially uniform state. The law is also independent of path, *i.e.*, E_c depends only on the specific distribution, not on how it was created. While here we evaluate the potential energy using (4.5) for an isolated drop, the result was originally derived for an arbitrary thin liquid layer with surfactant [45].

In Equation (4.5), c_0 is the instantaneous average value of the concentration on the drop

$$c_0(t) = \frac{1}{A_1}\iint c\,\mathrm{d}A_1\,.$$

Here $A_1(t)$ is the instantaneous 'footprint' area of the drop. W, the total work done in adding surfactant to the interface, may be found by summing the incremental changes in E_c over the period of injection, t_i say. The work is found by time integration of

$$\frac{\mathrm{d}W}{\mathrm{d}t} = \frac{\mathrm{d}E_c(t)}{\mathrm{d}t} = K\iint I(x, y, t)\,\log\frac{c}{c_0}\,\mathrm{d}A_1\,. \tag{4.6}$$

and I is given by (3.1) for example. Equation (4.6) follows immediately from the derived expression for ΔE_c in [45, p. 3091].

Inspection of the integrand in Equation (4.6) reveals that adding surfactant to the interface, at a place where c already exceeds the average value c_0 (as would be expected at the surfactant-production sites), increases the stored energy of the system. At these locations, I and $\log c/c_0$ are both positive. The total energy rate equation is

$$\dot{E}_c - \dot{E}_D = \dot{E}_d + \dot{E}_\sigma - \dot{E}_\mu \tag{4.7}$$

where $(\dot{})$ is equivalent to $\mathrm{d}/\mathrm{d}t$. The viscous rate of working may be shown to be equal to

$$\dot{E}_\mu = -\iint \mathbf{Q}\cdot\nabla p \ \mathrm{d}A = \iint p\nabla\cdot\mathbf{Q} \ \mathrm{d}A = -\iint p\, h_t \ \mathrm{d}A \tag{4.8}$$

in the long-wave approximation [29]. The last integral form is easily evaluated numerically, and p is given by (2.2). Equation (4.7) indicates that the net rate of energy increase due to surfactant addition, less diffusional surfactant energy losses along the surface and to the bulk liquid, denoting both by E_D, equals the disjoining energy rate increase and the capillary energy increase less the rate of viscous dissipation.

Energy-versus-time history plots are useful for tracking the progress of a splitting event. Such plots, for the splitting calculations of Figures 3–5, are shown in Figures 6 and 7. Figure 6 shows the dimensionless energy sum $\tilde{E} = \tilde{E}_d + \tilde{E}_\sigma$ for one-quarter of the quadrant-symmetric droplets shown in the rendered figures. The estimate, from (4.4) and recognizing that the unit of energy is σh_0^2, is $3\pi/4 \approx 2{\cdot}36$. For comparison, the calculated value, at the start of the motion, is 1·83. The estimated energy for two daughter droplets, from (4.4), is $2^{1/3}\ \tilde{E} \approx 2{\cdot}97$, an increase of about 26 per cent. The ultimate energy of the two daughter drops in the calculation is about 2·3 which, while smaller than the corresponding estimate, is larger than the starting energy $\tilde{E}$ by about the same factor. Note that the highly-distorted splitting of Figure 3 corresponds to a sharp peak of energy prior to relaxation. This case will be called the 'nominal case'. The cumulative surfactant-addition work for this case, in Figure 7, calculated using Equation (4.6) is relatively large. Because of the strong distortion as well as the dissipative mechanisms, the input work $\tilde{W} \approx 11$ is almost 25 times the minimum amount required to supply the increase in $\tilde{E}$.

Other cases, with even faster release of surfactant, can be compared, although not shown in the figures. A faster release of the same amount of surfactant will not produce breakage because the effect is dissipated too quickly. In the nominal test case, release ends at about $t = 0{\cdot}075$ when the source location has reached $x_0 = 0{\cdot}1$. Releasing the same total amount of surfactant, but at ten times the rate, only reduces the radius at the 'waist' to about 0·5 before all the surfactant is used up. The residual surface-tension gradient causes slight additional contraction at the waist and slight lengthening at expanding ends. However, once the driving force reduces somewhat, due to the diffusive mechanisms, the partially cleaved drop springs back to its original shape. Releasing surfactant at ten times the rate and maintaining the release until $x_0 = 0{\cdot}1$, as in the nominal case, causes faster break-up and the two daughters are slightly further apart at the end. With $C = 1000$, the surfactant stoppage condition is reached earlier, at $t = 0{\cdot}016$. About twice as much surfactant is used up compared to the nominal case. The distortion is even more violent than that shown in Figure 3, it clearly causes greater work to be done, and it also could cause internal damage if the process really were cell division.

More promising is slower release of surfactant as shown in Figure 4. Using $C = 5$ causes smooth, virtually quasi-static, distortion. The slow release allows the centers of the daughter drops to move apart simultaneously with waist contraction. This slow deformation results in

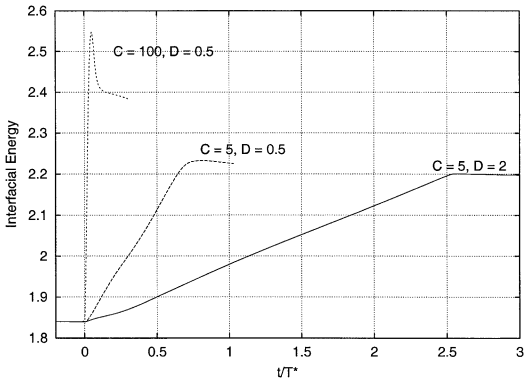

Figure 6. Dimensionless interfacial energy $\tilde{E}_d + \tilde{E}_\sigma$ versus dimensionless time for three combinations of surfactant supply rate C and surfactant diffusion $\tilde{D}$. Energy is measured in units of σh_0^2. $C = 100$ and $D = 0{\cdot}5$ is called the *nominal case* in the text. Each case for $\tilde{D} = 0{\cdot}5$ is a successful cleavage while the larger diffusion case results in a stretched and pinched drop that does not split. Because the calculation exploited the quadrant symmetry of the problem, energy values for the full problem are four times the values shown.

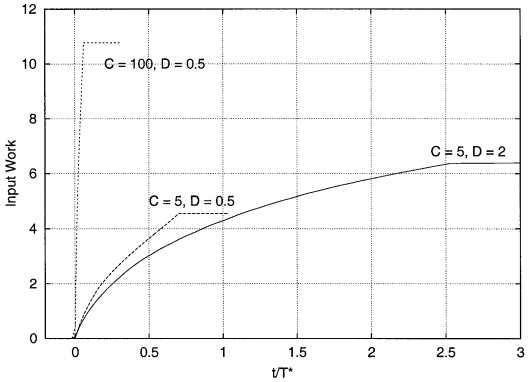

Figure 7. Cumulative surfactant injection work $\tilde{W}$ versus dimensionless time for the three cases in the previous figure. The units of work and energy are the same. Comparing the work input to the increase in interfacial energy yields a measure of the efficiency of the cleavage process, as discussed in the text. In each case, injection starts at time $t = 0$. According to the model, injection ceases when the surfactant sources come together.

a time-invariant driving concentration gradient pulling the daughters apart. Surfactant release stops at $t = 0{\cdot}7$. There is just enough residual Marangoni stress to complete the process. The corresponding energies are shown in Figures 6 and 7. The total surfactant injection work done, about 4·5 in dimensionless units, is much less than for the nominal case. Also shown in the energy plots is an unsuccessful cleavage because the surfactant diffusion rate is too large. This unsuccessful attempt used more work and more surfactant than the slow successful case. Clearly there is a 'working window' corresponding to gentle distortion and minimal requirements of energy and surfactant. This is what one would expect for a process that Nature has had a chance to optimize.

It can be shown that the time and energy measures in the current scenario appear to be reasonable. This is a type of test of the theory that has been made possible because we have a complete, albeit simple, mathematical process model. Figures 6 and 7 suggest that a typical time for cell division is about one characteristic time unit

$$T^* = \frac{3\mu R^4}{\sigma h_0^3} = 24\,\frac{\mu}{\sigma}\,\frac{R}{\theta_e^3} \tag{4.9}$$

where, assuming a paraboloidal drop, the approximate expression $\theta_e = 2h_0/R$ has been used. If we use typical values [43, 46, 18, 44], *i.e.*, σ = 1 dyne/cm, μ = 100 poise, $R = 5 \times 10^{-4}$ cm for a leukocyte and θ_e = 10 degrees $\approx 0{\cdot}2$ radian, the value of T^* is about 150 seconds which seems a plausible value. Times much smaller than this would have very large cell deformations, as in Figure 3 for example. Equation (4.9) indicates how this characteristic time would be changed if other liquid or cell properties were used instead.

Similarly, the energy associated with placing the necessary amount of surfactant on the interface can be compared with the associated amount of heating, using the mechanical equiv-

alent of heat. This assumes that the process work is ultimately converted to heat. The energy input to put surfactant that already exists in the bulk liquid onto the interface is not the only required energy; thus the amout of heating associated with this work should only increase the liquid temperature by a small fraction of a Celsius degree. If this were not true, then the envisioned process could be ruled out immediately because it would then be too expensive energetically. The specific heat of saline water is c $\approx 4 \times 10^7$ erg/gm/^{o}C. The temperature change ΔT due to energy addition E to a mass M is given by

$$\Delta T = \frac{E}{Mc} \,. \tag{4.10}$$

The mass of a paraboloidal sessile drop is $M = (\pi/2)\rho R^2 h_0$. A representative and quite adequate measure of the input work, from Figure 7, is $E = 4(10)\,\sigma h_0^2$. Then, with $\theta_e = 2h_0/R$, one obtains

$$\frac{E}{Mc} = \frac{80}{\pi}\,\frac{\sigma h_0}{\rho R^2 c} = \frac{40}{\pi}\,\frac{\sigma\,\theta_e}{\rho R c} \,. \tag{4.11}$$

Using the leukocyte radius $R = 0{\cdot}0005$ cm, and the values σ = 1 dyne/cm, $\rho = 1$ gm/cm^3 and $\theta_e = 10^o = 0{\cdot}.2$ radian, the temperature increase is only 10^{-4} °C. Even if the radius were reduced by a factor of 100 for very small cells, *e.g* mycoplasma, ΔT would still only be 0·01 °C. Thus the energy requirements for this process appear to be suitably small.

5. Motility

Motility refers to the ability of a cell, or single cell animal such as an amoeba, to move under a self-supplied driving force. We have seen that insufficient surfactant release, or release at too slow a rate, will cause a drop or cell to distort without dividing. It is also possible to use relatively low levels of surfactant production to move the drop/cell from one position on the substrate to another. In this way, motility may simply be a special case of division; one that happens by essentially the same surfactant release mechanism, namely a net surface traction due to nonuniform surfactant distribution. More generally, this is an example of droplet motion driven by surface tension gradients. Such gradients can also result from temperature gradients and a number of theoretical and experimental studies of such motions have appeared [47–49].

Amoeboid motion is usually described as proceeding in steps: the animal sticks out a foot or pseudopod, somehow draws cellular material along the foot, and ultimately reforms into the original shape at the new location selected by the starting foot. Simulation results below roughly approximate this type of motion, both in two and three dimensions.

The equations governing the motion are still the coupled system (2.9)–(2.12). Unlike splitting scenarios, where surfactant is released on opposite sides, for motility surfactant is released at the 'back', *i.e.*, the end opposite the one that moves forward. Here we merely demonstrate that motility is possible using surfactant release. Compared with amoeba motion however, we are basically pushing from the back while, arguably, the amoeba moves forward primarily by 'pulling from the front'.

Figure 8 shows results from a two-dimensional simulation. Parameter values are as before, except that the surfactant strength parameter is $R = 25$ rather than 100. A fine mesh is used for the calculation. The starting drop shape is the equilibrium parabola with no surfactant injection. The injection is stopped at $t/T^* = 50$. Note that, while moving, the drop is lengthened relative to its rest length. In the motion shown in the figure, the drop moves a distance equal

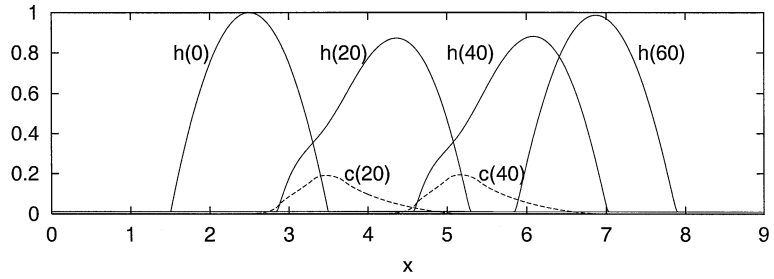

Figure 8. A two-dimensional simulation of cell or drop motility. Four profiles $h(x, t)$ are shown at the dimensionless times $t = 0$, 20, 40 and 60. Surfactant release is started at $t = 0$ near the back of this 2D sessile drop. This release continues at a constant rate until $t = 50$ when it is turned off. A steadily propagating shape, moving from left to right at constant speed, is soon formed. Surfactant profiles are shown superimposed at $t = 20$ and 40. After surfactant release stops, the surfactant is dissipated, the drop re-forms to its original shape, and it stops moving.

to more than twice its rest length. A somewhat shorter excursion, which would be produced if the surfactant release were turned off earlier, could arguably be described by the three-step ameboid motion given above.

Results of a three-dimensional calculation for surfactant-driven motility are shown in the following two figures. The droplet is first allowed to relax to its equilibrium shape. Then, at $t/T^* = 0$, surfactant release is started and continues at a constant rate, until $t/T^* = 10$ when it is turned off. The surfactant quickly dissipates and the droplet, having moved a distance of about six-tenths of a diameter, relaxes again to the equilibrium shape. Figure 9 show contour plots of h and c superimposed at various times. The contour levels for h are 0·06, 0·1, 0·2, 0·3 and 0·4 while the contour levels for c are 0·02, 0·040 and 0·06. Figure 10 shows rendered pictures of the drop at two dimensionless times: $t = 6$ and $t = 10$. As surfactant is released near the back of the drop, the profile becomes inclined forward, in the direction of motion.

6. Concluding remarks

There are three purposes for this paper. First, it is meant to enumerate all of the components required for a logically complete mathematical model for liquid layer motion, with surfactant effect, on a substrate in three space dimensions. Very many simplifying assumptions have been invoked in order to make the problem tractible. Secondly, we demonstrate the feasibility of calculating model results using an ADI method. Finally, we propose, or more correctly *revisit*, a particular theory of cell division. We also demonstrate that the same mechanism can be used by the cell for self propulsion.

The mechanism is the production of surfactant and its introduction, in some way, into the free surface or cell membrane. In a sense this is the simplest possible mechanism for division. We know that cells have the ability to make surfactant and also to insert the surfactant onto their bounding membranes. The membranes are surfactant-laden bilayers and the total surface area must increase when cells divide. In the present version of the surfactant release theory, it is simply the Marangoni force that results from spatially nonuniform addition of surfactant that causes the splitting. The main purpose of the numerical calculation is to demonstrate that the Marangoni force is sufficient to cause splitting using plausible physical input parameter values.

Certain input parameters are gross estimates. For example, the two dissipative mechanisms, Fickian diffusion of surfactant on the surface and exchange of surfactant with the bulk liquid,

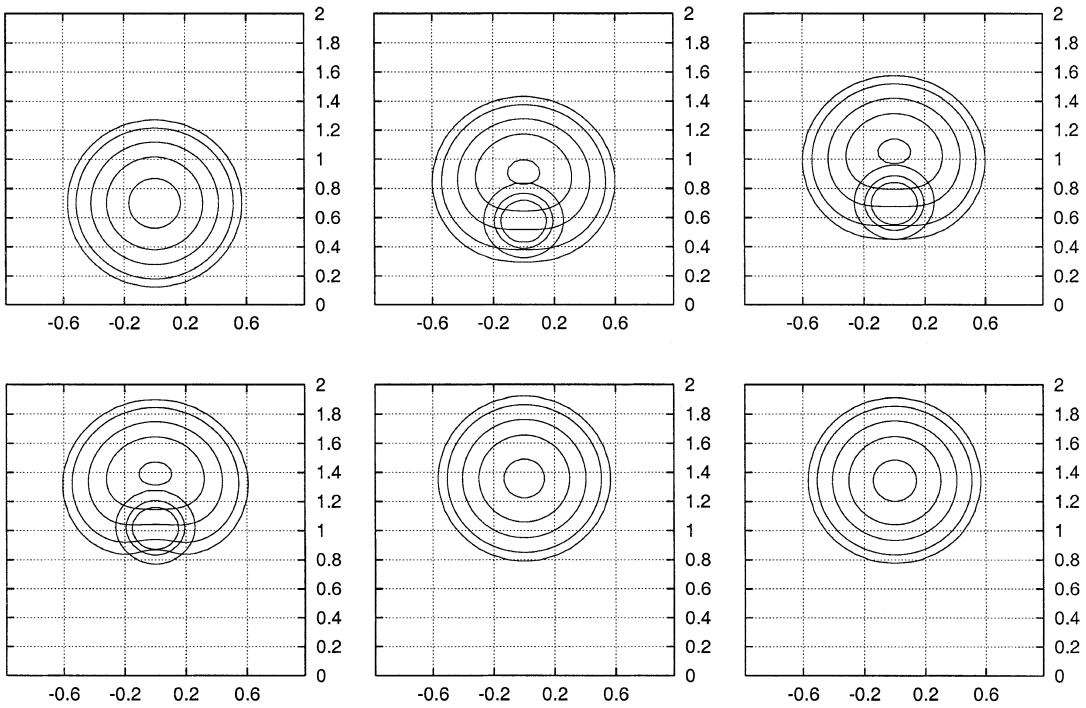

Figure 9. Results of a motility calculation. Surfactant release is used to drive droplet motion. Contour plots of surface height (large pattern) and surfactant concentration (small pattern) at time $t = 0$, 3·5, 6, 10, 11 and 13. The contour levels and other parameter values are given in the text. The nominal drop radius and central height are each equal to 0·5. The general direction of motion is upward in the figures (read across, then down). The surfactant has not yet been introduced at $t = 0$. The surfactant has been sensibly dissipated by $t = 11$. Between $t = 11$ and $t = 13$, the drop steepens slightly, returning to its original ($t = 0$) shape.

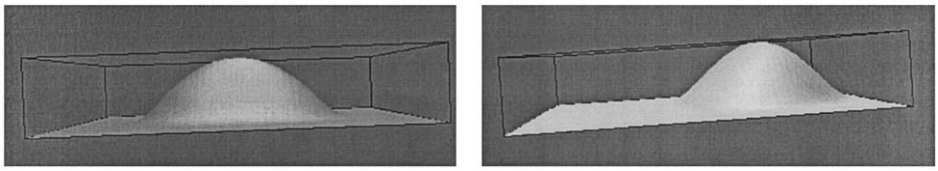

Figure 10. Rendered pictures of two drop shapes shown in the contour plots above. Here $t = 6$ (left) and 10 (right). The drop is moving from left to right in these two pictures. The drop shape is not axisymmetric. For example, the highest point on the drop is leaning somewhat in the direction that the drop is moving.

require the specification of rate constants that are not known to us. We have explored a range of values. By comparing the stored energy and work histories in Figures 6 and 7, we see that our range corresponds to efficiencies between about five and fifteen per cent. Nevertheless, in contrast with previous modeling attempts, we show that drop or cell division can be made to happen quite readily, within the model, and that slower processes are more favorable from an efficiency viewpoint. In addition, an order-of-magnitude calculation is offered to establish that the surfactant injection work required for cell division or motility would only lead to a temperature increase that is a small fraction of one Celsius degree.

Acknowledgment

This work is partially supported by The ICI Strategic Research Fund. Previous work, on closely-related topics, was supported by The NASA Microgravity Program and The State of Delaware through The Delaware Research Partnership Program.

References

1. I.B. Ivanov (ed.), *Thin liquid films; Fundamentals and Applications*. New York: Marcel-Dekker (1988) 1126 pp.
2. B. Warburton, Interfacial rheology. *Cur. Opinion in Colloid Interf. Sci.* 1 (1996) 481–487.
3. K. Mysels, K. Shinoda and S. Frankel. *Soap Films, Studies of their Thinning*. New York: Pergamon (1959) 116 pp.
4. P.L. Evans, L.W. Schwartz and R.V. Roy, A mathematical model for crater defect formation in a drying paint layer. *J. Colloid Interf. Sci.* 227 (2000) 191–205.
5. D.E. Weidner, L.W. Schwartz and R.R. Eley, Role of surface tension gradients in correcting coating defects in corners. *J. Colloid Interf. Sci.* 179 (1996) 66–75.
6. S.D. Howison, J.A. Moriarty, J.R. Ockendon, E.L. Terrill and S.K. Wilson, A mathematical model for drying paint layers. *J. Engng. Math.* 32 (1997) 377–394.
7. D.J. Benney, Long waves on liquid films. *J. Math. Phys.* 45 (1966) 150–155.
8. R.W. Atherton and G.M. Homsy, On the derivation of evolution equations for interfacial waves. *Chem. Engng. Comm.* 2 (1976) 57–77.
9. E.O. Tuck and L.W. Schwartz, A numerical and asymptotic study of some third-order ordinary differential equations relevant to draining and coating flows. *SIAM Rev.* 32 (1990) 453–469.
10. L.W. Schwartz and H.M. Princen, A theory of extensional viscosity for flowing foam. *J. Colloid Interf. Sci.* 118 (1987) 201–211.
11. D.P. Gaver and J.B. Grotber, The dynamics of a localized surfactant on a thin film. *J. Fluid Mech.* 213 (1990) 127–148.
12. A. De Wit, D. Gallez and C.I. Christov, Nonlinear evolution equations for thin liquid films with insoluble surfactant. *Phys. Fluids* 6 (1994) 3256–3266.
13. L.W. Schwartz, D.E. Weidner and R.R. Eley, An analysis of the effect of surfactant on the leveling behavior of a thin liquid coating layer. *Langmuir* 11 (1995) 3690–3693.
14. J.B. Grotberg and D.P. Gaver, A synopsis of surfactant spreading research. *J. Colloid Interf. Sci.* 178 (1996) 377–378.
15. D.W. Peaceman and H.H. Rachford, Jr., The numerical solution of parabolic and elliptic differential equations. *SIAM J.* 3 (1955) 28–41.
16. S.D. Conte and R.T. Dames, On an alternating direction method for solving the plate problem with mixed boundary conditions. *J. Assoc. Comp. Mach.* 7 (1960) 264–273.
17. N.N. Yanenko, *The Method of Fractional Steps.* New York: Springer-Verlag (1971) 160 pp.
18. H.P. Greenspan, Dynamics of cell cleavage. *J. Theor. Biol.* 65 (1977) 79–99.
19. H.P. Greenspan, On the deformation of a viscous droplet caused by variable surface tension. *Stud. Appl. Maths.* 57 (1977) 45–58.
20. H.P. Greenspan, On fluid-mechanical simulation of cell division and movement. *J. Theor. Biol.* 70 (1978) 125–134.
21. H.P. Greenspan, On the motion of a small viscous droplet that wets a surface. *J. Fluid Mech.* 84 (1978) 125–143.
22. R. Rappaport, *Cytokinesis in Animal Cells*. Cambridge: Cambridge Univ. Press (1996) 386 pp.
23. A.N. Frumkin, On the phenomena of wetting and sticking of bubbles. *Zhurnal Fizicheskoi Khimii* 12 (1938) 337 (In Russian).
24. B.V. Derjaguin. Theory of the capillary condensation and other capillary phenomena taking into account the disjoining effect of long-chain molecular liquid films. *Zhurnal Fizicheskoi Khimii* 14 (1940) 137 (in Russian).
25. N.V. Churaev and V.D. Sobolev, Prediction of contact angles on the basis of the Frumkin-Derjaguin approach. *Adv. Colloid Interf. Sci.* 61 (1995) 1–16.

26. V.S. Mitlin and N.V. Petviashvili. Nonlinear dynamics of dewetting: Kinetically stable structures. *Physics Letters: Part A* 192(5–6) (1994) 323–326.
27. L.W. Schwartz, Unsteady simulation of viscous thin-layer flows. In: P. Tyvand (ed.), *Free Surface Flows with Viscosity*. Southampton, 1997: Computational Mechanics Publications, pp. 203–233.
28. L.W. Schwartz, Hysteretic effects in droplet motions on heterogeneous substrates: Direct nummerical simulation. *Langmuir* 14 (1998) 3440–3453.
29. L.W. Schwartz and R.R. Eley, Simulation of droplet motion on low-energy and heterogeneous surfaces. *J. Colloid Interf. Sci.* 202 (1998) 173–188.
30. A. Sharma, Equilibrium and dynamics of evaporating or condensing thin fluid domains: thin film stability and heterogeneous nucleation. *Langmuir* 14 (1998) 4915–4928.
31. C. Huh and L.E. Scriven, Hydrodynamic model of steady movement of a solid/liquid/fluid contact line. *J. Colloid. Interf. Sci.* 35 (1971) 85–101.
32. J. Spek, Oberflachenspannungensdifferenzen als eine Ursache der Zellteilung. *Arch. f. Entwick-lungs Mech.* 44 (1918) 5–113.
33. X. He and M. Dembo, Numerical simulation of oil droplet cleavage by surfactant. *J. Biomech. Engng.* 118 (1996) 201–209.
34. D. Zimmerman and A. Nir, On the viscous deformation of biological cells under anisotropic surface tension. *J. Fluid Mech.* 193 (1988) 217–241.
35. S.B. Carter, Haptotaxis and the mechanism of cell motility. *Nature* 213 (1967) 256–260.
36. D. Marsland and J.V. Landau, The mechanisms of cytokinesis. *J. Exp. Zool.* 125 (1954) 507–539.
37. L.D. Landau and E.M. Lifshitz, *Fluid Mechanics*. Oxford: Pergamon Press (1959) 536 pp.
38. V.G. Levich, *Physiochemical Hydrodynamics*. Englewood Cliffs: Prentice-Hall, Inc. (1962) 700 pp.
39. H.A. Stone, A simple derivation of the time-dependent convection-diffusion equation for surfactant transport along a deforming interface. *Phys. Fluids (A)* 2 (1990) 111.
40. H. Wong, D. Rumschnitzki and C. Maldarelli, On the sufactant mass balance at a deforming fluid interface. *Phys. Fluids* 8 (1996) 3203–3204.
41. L.W. Schwartz, R.A. Cairncross and D.E. Weidner, Anomalous behavior during leveling of thin coating layers with surfactant. *Phys. of Fluids* 8 (1996) 1693–1695.
42. M.H. Eres, D.E. Weidner and L.W. Schwartz, Three-dimensional direct numerical simulation of surface-tension-gradient effects on the leveling of an evaporating multi-component fluid. *Langmuir* 15 (1999) 1859–1871.
43. E.N. Harvey, Tension at the cell surface. *Protoplasmatologia* IIE5 (1954) 1–30.
44. R.M. Hochmuth, Micropipette aspiration of living cells. *J. Biomech.* 33 (2000) 15–22.
45. L.W. Schwartz and R.V. Roy, Some results concerning the potential energy of interfaces with nonuniformly distributed surfactant. *Phys. Fluids* 13 (2001) 3089–3092.
46. D. Branton and D.W. Deamer, Membrane structure. *Protoplasmatologia* II (1972) 1–70.
47. D.M. Cazabat, F. Heslot, S.M. Troian and P. Carles, Fingering instability of thin spreading films driven by temperature gradients. *Nature* 346 (1990) 824–826.
48. M.K. Smith, Thermocapillary migration of a two-dimensional droplet on a solid surface. *J. Fluids Mech.* 294 (1995) 209–230.
49. S.W. Benintendi and M.K. Smith, The spreading of a nonisothermal liquid droplet. *Phys. Fluids* 11 (1999) 982–989.